Study of Noise on a Small-Scale Hovering Tilt Rotor

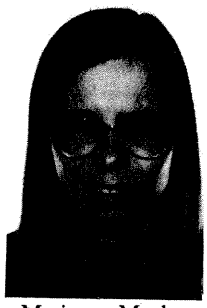

Marianne Mosher

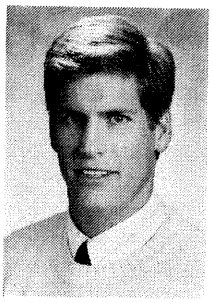

Jeffrey S. Light

Aerospace Engineers
NASA Ames Research Center

A study of the noise from a small-scale, semi-span test of a hovering tilt rotor is presented. The effect on noise of the tilt rotor fountain and of several tilt rotor configuration changes is examined. Measurements were made of an isolated rotor; rotor and wing; rotor and image plane; and rotor, wing and image plane. This last configuration models a tilt rotor. With a tilt rotor, the wing turns some of the rotor downwash inboard. When the flows meet, some of the flow is forced upward creating a fountain. Some of the fountain is ingested into the rotor disc. Rotor fountain interactions produce very unsteady impulsive noise to the rear of the aircraft. Configuration changes to investigate download reduction included increasing the rotor/wing separation, deflecting the flap, adding the nacelle, adding vortex trapping plates and blowing on the upper surface. These configuration changes produced little or no effect on the noise, although they changed the net download. Increasing the wing span, however, reduced the annoying content of this impulsive noise about 2 dB.

Notation

A	Rotor disk area, ft^2
BL-SPL	Band limited overall sound pressure level, power summed from 445 to 4490 Hz, dB referenced to 20 μPa
C_{TE}	Effective thrust coefficient, $(T\text{-}DL)/(\rho AV_{tip}^2)$
DL	Download on wing, lb
FA-SPL	A- weighted sound pressure level, adjusted to full-scale frequency, dbA referenced to 20 μPA
M_{tip}	Rotor tip Mach number
OASPL	Overall sound pressure level, dB referenced to 20 μPA
T	Rotor thrust, lb
V_{tip}	Rotor tip speed, ft/s
ρ	Air density, $slug/ft^3$
ψ	Azimuth angle, referenced to 0 deg over centerline of aircraft tail, deg

Introduction

The development of tilt rotors for civil transport provides an opportunity to improve short range air transportation for trips of less than 500 miles. Tilt rotors can operate out of heliports to offer a convenient method of inter-city transportation in the future. Designing and operating tilt rotors with low noise in terminal areas is a major challenge to the development of civilian tilt rotors. Although noise on approach due to blade vortex interaction is a primary concern for tilt rotors, noise in hover can also be detrimental to acceptance of this aircraft.

Tilt rotors in hover produce noise from the same sources as a helicopter main rotor in hover, in addition to noise caused by the rotor blades interacting with the fountain flow. The fountain, identified and described in Ref. 1, occurs when downwash from the two rotors hits the wings, which turn some of this flow toward the center of the aircraft. When these flows meet, some of the flow is forced upward to form a fountain. As the rotor blades ingest the fountain and interact with the disturbances, rapid pressure fluctuations occur on the blades and radiate as sound. The pressure fluctuations create large disturbances that radiate mostly perpendicular to the rotor blade. Due to convective amplification, the vertical dipole radiation pattern rotates aft, since the rotors move from front to aft inboard where they interact with the fountain. The additional forces include periodic forces due to the average fountain flow and unsteady forces from turbulence and unsteadiness in the fountain. Thus the acoustic field radiated from a hovering tilt rotor is expected to be greater than the acoustic field radiated from two equivalent non-interacting hovering helicopter rotors. Refs. 1 to 5 describe work on the basic flow field of a tilt rotor in hover. Refs. 5 and 6 describe the fundamental acoustic mechanisms for a tilt rotor in hover. Refs. 7 and 8 report on noise measurements of a XV-15 aircraft in hover, including identifying the directivity pattern of the impulsive hover noise from blade/fountain interactions. Some computations of this noise have been attempted in Refs. 5 and 9 to 11.

This paper describes an experimental study of the noise created by a rotor interacting with a fountain. Noise measurements from a small-scale, semi-span tilt rotor model are shown, including the effects of several configurations tested for their potential to reduce download. Time histories, spectra, and average noise metrics are presented.

Experiment

Test Hardware

A test was conducted at the NASA Ames Outdoor Aerodynamic Research Facility to examine tilt rotor wing download and noise (Ref. 12). Test hardware included a 7/38-scale V-22 rotor, a V-22 wing and an image plane (Fig. 1). The rotor, wing, and image plane were installed in a nominal V-22 configuration: the wing had 6 deg forward sweep, 3.5 deg dihedral, and 85 deg incidence to the flow from the rotor. These angles, as well as the spacing between the rotor, wing, and image plane

Presented at the American Helicopter Society Aeromechanics Specialists Conference, San Francisco, California, Jan. 19-21, 1994.

Manuscript received Sept. 1994; accepted Jan. 1996.

were adjustable. Tables 1 and 2 list characteristics of the rotor and wing, respectively. The image plane was 12 ft high by 16 wide (3.658 by 4.877 m); it was not large enough to reflect the acoustic image to the microphone locations. The discussion section tells more about the image plane. An open support structure around the rotor held the wing and its balances in place. The rotor/wing setup allowed the rotor wake to convect up into the wing. The rotor rotation direction causes the blades to pass over the wing leading edge before the wing trailing edge. All discussions of up and down in the remainder of the paper will refer to regular aircraft directions. A model nacelle was also included in some runs to determine its effect on download and acoustics. The changes in noise for changes in baseline V-22 geometry and two potential download reduction techniques were also examined. The first, vortex trapping plates, consisted of two spanwise plates mounted on the wing upper surface. The second, upper surface blowing, blew air out of spanwise slots on the wing upper surface. Microphones were placed 7 rotor radii from the rotor hub and 45 deg below the rotor plane, as defined in aircraft terms. Microphone 1 is forward (ψ=180 deg) of the wing and microphone 2 is aft (ψ=0 deg) of the wing. The microphone locations were based on earlier full-scale measurements (Ref. 7) which identified the location 45 deg below the rotor plane and behind the aircraft as a location with high levels of noise from the rotor interacting with the fountain. Foam was placed on the ground between the rotor and the microphones to reduce spurious reflections.

Table 1. Rotor Characteristics

Number of blades	3
Rotor radius	3.5 ft (1.067 m)
RPM	2074 to 2112
BPF	103.7 to 105.6 Hz
M_{tip}	0.684 to 0.688
Mean blade chord	0.45 ft (0.137 m)
Rotor solidity ratio	0.1138
Blade twist, nonlinear	-34.08 deg
Blade Precone	1.5 deg
Blade Airfoils	XN-28, XN-18, XN-12, XN-09

Table 2. V-22 Wing Characteristics

Wing airfoil section	Bell A821201
Wing chord	1.54 ft (0.469 m)
Wing thickness ratio	23%
Wing twist	0 deg
Wing dihedral	0 deg, 3.5 deg
Wing sweep	0 deg, -6 deg
Flap chord ratio	30%
Distance from wing chord line to rotor hub	18.125, 29.375 in (0.460, 0.746 m)
Distance from wing leading edge to rotor hub	10.125 in (0.257 m)
Distance from wing tip to rotor hub	3.938 in (0.100 m)
Wing span (rotor centerline to image plane)	51.625, 58.125 in (1.311, 1.476 m)

Instrumentation

A load cell balance in the base of the test stand and a flexible shaft coupling measured rotor forces and moments. Wing download measurements were obtained using two balances, one in each arm of the support structure. Wind speed was measured with a cup anemometer. Bearing friction in the anemometer caused inaccurate wind measurements below 3 knots. Acoustic pressures were measured with 0.5-in condenser microphones with windscreens. Individual power supplies were used to control the gain on each microphone. Signals were monitored on an oscilloscope and recorded on a 14-track FM tape recorder running at 30 in per second in Wide Band I.

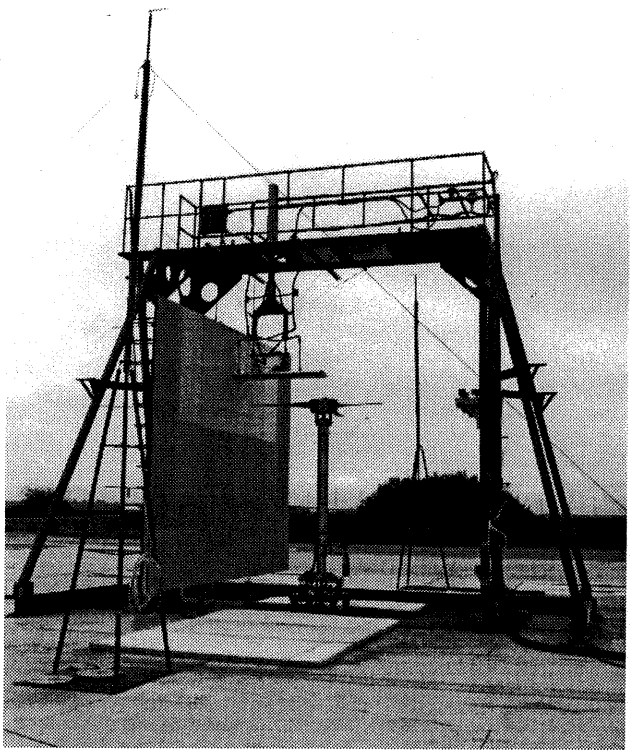

Fig. 1. Test hardware at Outdoor Aerodynamics Facility.

Testing Process

The rotor was operated at a full-scale tip Mach number of 0.686. Acoustic data were acquired for the thrust coefficient-to-solidity ratios of 0.010 to 0.016. Measurements were made in the early morning to obtain the lowest wind speeds; the wind was always below 5 knots. Performance and download data were averaged over 10 seconds at each operating condition. About 30 seconds of acoustic data were recorded on analog tape. Performance, download and acoustic records were recorded at the same time, but were not synchronized with each other. Ref. 12 describes the test.

Data Analysis

Eight seconds of acoustic pressures were digitized with the ALDAS program (Ref. 13) on a computer with 12 bit A/D boards. The digitization rate was 15,384 Hz. Due to the high peak-to-peak amplitude, the acoustic spectra above about 4 to 5 kHz are contaminated by the noise floor of the analog tape recorder.

Time histories of acoustic pressure were examined. In many individual data records, the time histories contain impulses of widely varying amplitude, shape and location; these variations occur from blade to blade and revolution to revolution. For these very unsteady conditions, time histories are shown which are representative of very low amplitude and very high amplitude for that time record. Synchronously averaged time histories were also produced by using a 1/rev signal as a trigger.

To compare the sound from various configurations, several acoustic metrics were computed from 8 second time histories containing over 250 revolutions. Spectra were produced by averaging 60 power spectra made from blocks of data 2048 samples long with a Hanning window. From the averaged power spectra the overall sound pressure level (OASPL), band limited overall sound pressure level (BL-SPL) and a frequency adjusted A-weighted sound pressure level (FA-SPL) were

calculated. OASPL emphasizes the acoustic energy in the first few blade passage harmonics. The BL-SPL contains the linear sum of the acoustic energy from the frequencies spanning 445 to 4490 Hz (includes blade passage harmonics number 5 through 42). This removes from the OASPL the first 4 blade passage harmonics and the high frequency energy contaminated by the analog tape recorder. BL-SPL emphasizes the energy associated with the impulsive noise caused by the rotor/fountain interaction or the mid-frequency range of the spectrum when the fountain is not present. The FA-SPL applies the A-weighting to the spectrum scaled to the full-scale frequencies. FA-SPL emphasizes human perception of the noise.

Since the tip Mach number was kept constant, the rotor thrust was the main operating parameter expected to affect the noise. Variations in wind and atmospheric turbulence can also be expected to affect the sound levels. All measurements were made under calm conditions with the wind below 5 knots. A statistical analysis of the measurements revealed no correlation between the acoustic measurements and the wind speed. For comparisons, the acoustic metrics are plotted against the effective thrust coefficient. The effective thrust is based on the difference between rotor thrust and wing download.

To examine the unsteadiness in the acoustic measurements, the OASPL, BL-SPL and FA-SPL were also computed for each revolution from a short-time Fourier analysis. A Fourier transform was applied to each revolution without any windowing. Results show significant variability between revolutions, more than 5 dB in some cases. The long record length, over 250 revolutions, is long enough to produce a stable average.

Results

Time histories, spectra and average noise metrics are presented for the following configurations: rotor; rotor and support structure; rotor and image plane; rotor and wing; and rotor, wing and image plane. Results for different wing configurations are also presented. Figures that show acoustic metrics as a function of effective thrust coefficient contain all available data.

Isolated Rotor and Support Structure

Acoustic measurements of the isolated rotor resemble typical noise from a hovering rotor at high thrust. Fig. 2 shows a time history measured at location 2, to the rear of the model, for one rotor revolution. Fig. 3 shows a 7.5 Hz narrow band averaged power spectra of this typical condition. The tip Mach number is 0.686 and the effective thrust coefficient is 0.0130. The first harmonic of the blade passage frequency dominates the signal. The amplitude and general shape of the signal remain fairly constant over the 8 seconds analyzed. The time history varies slightly from blade-to-blade and revolution-to-revolution. Fig. 4 shows time histories of the OASPL, BL-SPL and FA-SPL computed for the first 250 revolutions measured during the 8-second record. Small variations of about 1 dB in the OASPL indicate the energy in the dominant first harmonic is very steady over the approximately 8-second record. Larger variations of about 5 dB occur in the BL-SPL and FA-SPL. The BL-SPL and FA-SPL include noise from atmospheric turbulence ingestion. These time histories are stochastic over the 250 revolutions, so the metrics computed from the 8 second records are considered valid measurements characterizing the sound from the hovering rotor.

The support structure for the wing produced no measurable effect on the sound measured at the two microphone locations. Figs. 5 a and b show OASPL and FA-SPL, respectively, measured at both locations as a function of effective thrust coefficient. The tip Mach number ranged from 0.684 to 0.686 and the wind was less than 5 knots. Unfortunately, minimal overlap of thrust coefficients exists between the two configurations. The discussion section includes some comments about this. The data contain a considerable amount of scatter, up to 5 dB over the 8 second records. A tail rotor, similar in size to the rotor in this study, was also tested at the Outdoor Aerodynamic Research Facility under low wind conditions (Ref. 14). At low thrust, the scatter seen in noise measurements of this tilt rotor is similar to the scatter seen in noise measurements of the other rotor in Ref. 14. At high thrust levels the scatter seen in this tilt rotor exceeds that seen in the other rotor by about 50 percent. Fig. 5 shows that within the scatter, noise measurements are approximately the same at both locations and with or without the sup-

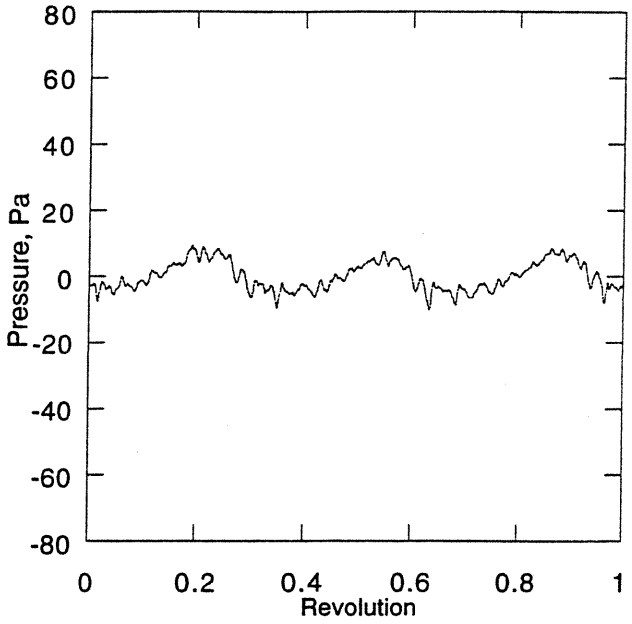

Fig. 2. Typical unaveraged time history of the isolated rotor, microphone 2, C_{TE} = 0.0130, M_{tip} = 0.686.

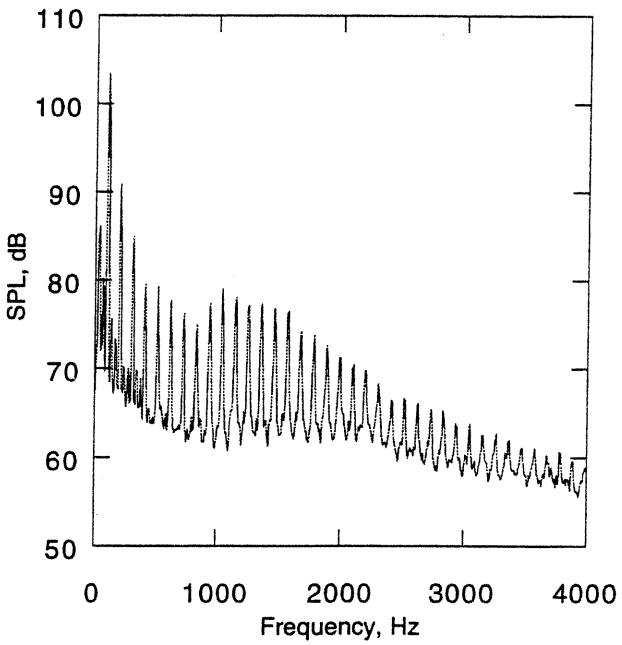

Fig. 3. Averaged power spectrum of the isolated rotor, microphone 2, C_{TE} = 0.0130, M_{tip} = 0.686, ΔF = 7.5 Hz.

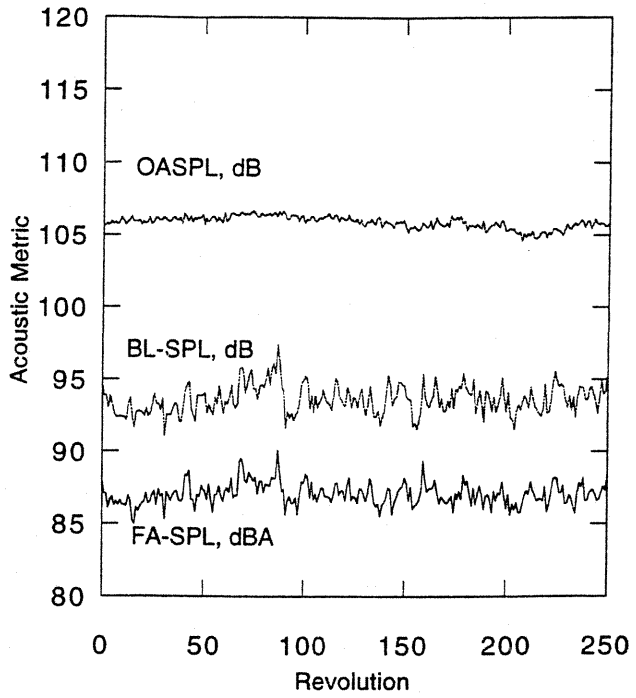

Fig. 4. Acoustic metrics for the isolated rotor, microphone 2, C_{TE} = 0.0130, M_{tip} = 0.686.

port structure. For noise mechanisms whose amplitude is proportional to thrust, the amplitude is expected to increase about 4 dB over the thrust increase of 60 percent (from 0.01 to 0.016). Within the scatter, noise levels increase with thrust by this expected amount.

Rotor and Image Plane

Adding the image plane to the isolated rotor increases the overall noise levels by about 2 dB and the A-weighted frequency scaled levels by about 5 dBA. Figs. 6 a and b show unaveraged time histories of acoustic pressure for a revolution with low amplitude and a revolution with high amplitude, respectively, measured to the rear of the model (microphone 2). Test conditions are nearly the same as for the example with the rotor alone (Fig. 2). The image plane changed the inflow to the rotor creating a disturbance at the rotor which radiates as a small impulse in the wave form. The averaged power spectrum in Fig. 7 shows an increase in amplitudes of blade passage harmonics above the second harmonic. Fig. 8 shows time histories of the OASPL, BL-SPL and FA-SPL computed for 250 revolutions. Comparison of Figs. 4 and 8 show that the isolated rotor noise levels are lower than the noise from the rotor plus image plane. The variation is about the same. Acoustic pressures measured in front of the model (microphone 1) are also higher and have the same characteristics as the isolated rotor. In front of the rotor, the fundamental blade passage harmonic dominates.

Rotor and Wing

Adding the semi-span wing to the isolated rotor increases the overall noise levels about 2 dB and the A-weighted frequency scaled levels about 5 dBA. The variation in levels among different revolutions of a data record also increases. For these results, the wing is in the baseline V-22 configuration with 0 deg flap setting. Figs. 9 a and b show unaveraged time histories of acoustic pressure for a revolution with low amplitude and high amplitude, respectively, measured to the rear of the model (microphone 2) from the same data record. Tip Mach number is the same as for the results with the rotor alone (Fig. 2). Rotor thrust is increased 7 percent to compensate for the download. Like the

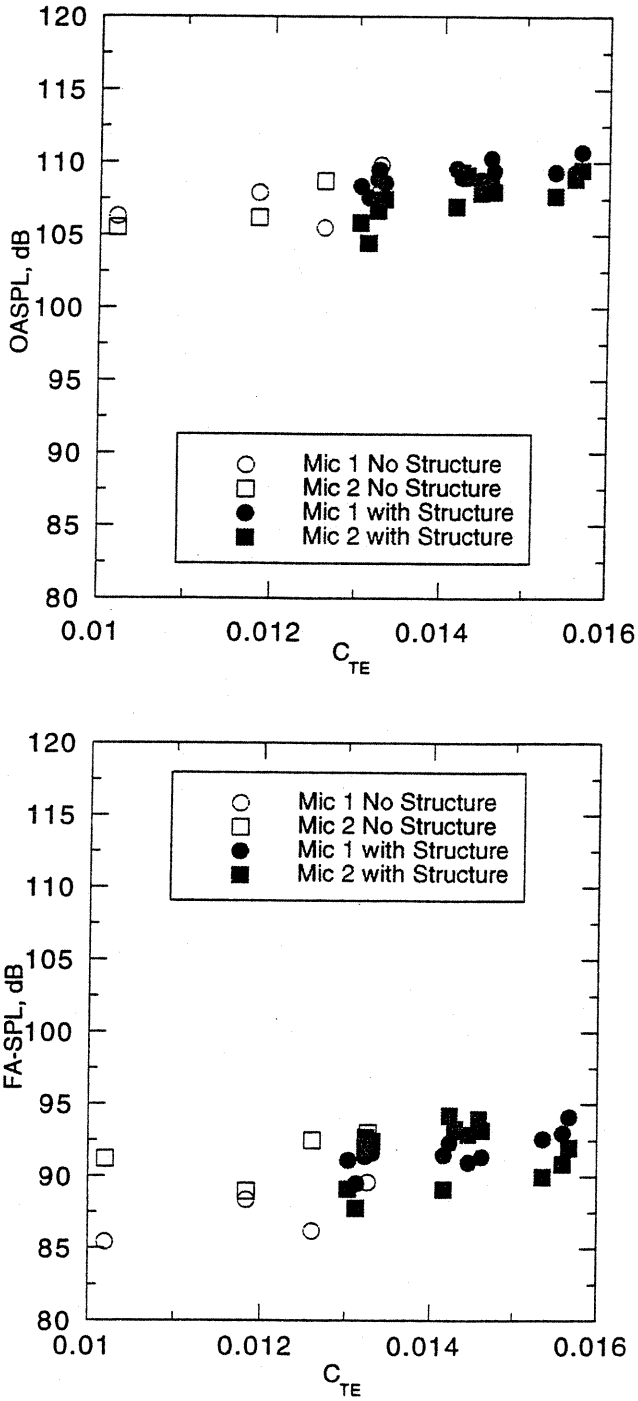

Fig. 5. Sound levels for isolated rotor with and without wing support structure (a) OASPL; (b) FA-SPL.

image plane, the wing also introduces a disturbance to the rotor inflow that appears as a small impulse in the wave form. The averaged power spectrum in Fig. 10 shows an increase in amplitude of a few dB at the lower blade passage harmonics and 8 to 10 dB above the 4th harmonic compared to the isolated rotor. Fig. 11 shows time histories of the OASPL, BL-SPL and FA-SPL computed for 250 revolutions. Levels are higher compared to the rotor alone case and the variation is somewhat greater. Acoustic pressures measured in front of the model (microphone 1) are also higher with the wing added and have similar characteristics to the isolated rotor. In front of the rotor, the time histories sometimes contain small impulses.

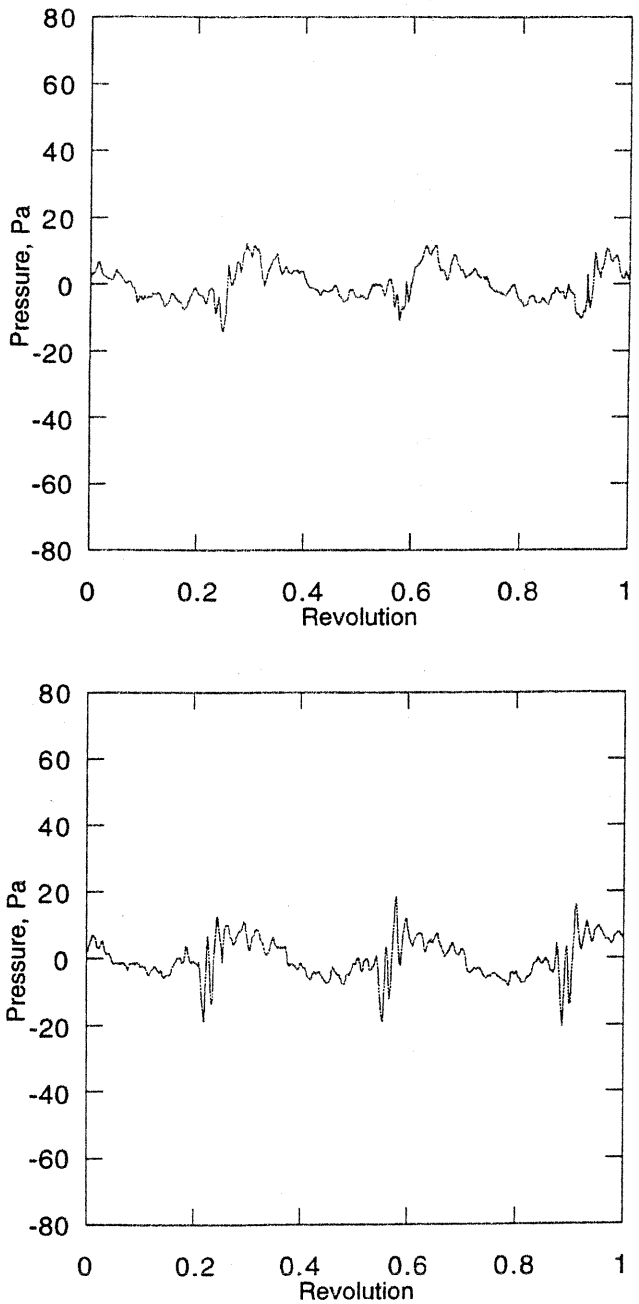

Fig. 6. Unaveraged time histories measured at the rear of the rotor with image plane, microphone 2, C_{TE} = 0.0131, M_{tip} = 0.685 (a) low amplitude (b) high amplitude.

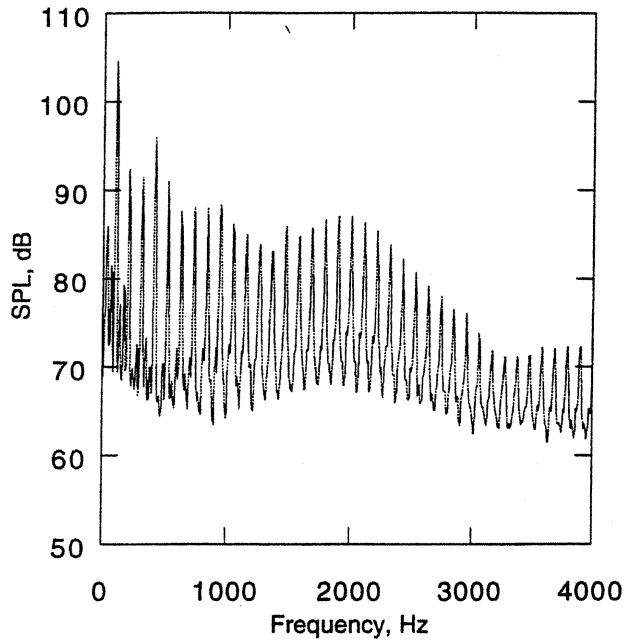

Fig. 7. Averaged power spectrum for the rotor with image plane, microphone 2, C_{TE} = 0.0131, M_{tip} = 0.685, ΔF = 7.5 Hz.

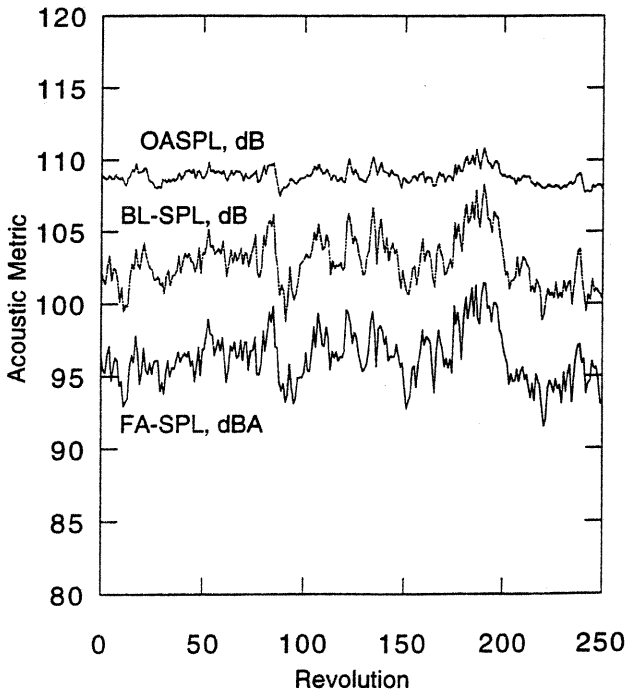

Fig. 8. Acoustic metrics for the rotor with image plane, microphone 2, C_{TE} = 0.0130 M_{tip} = 0.685.

Rotor, Wing and Image Plane

Adding both the wing and image plane to the rotor approximately simulates the aerodynamics of the full tilt rotor configuration including the addition of a fountain to the flow. The flow field with an image plane lacks the shifting of the fountain noted in Ref. 3. Overall noise levels increase about 4 dB and the A-weighted frequency scaled levels increase about 10 dBA compared to the isolated rotor. The variation in levels among different revolutions of a data record increases. Figs. 12 a, b, and c show unaveraged time histories of acoustic pressure for a revolution with low amplitude, high amplitude and a synchronous average of 60 revolutions, respectively, measured to the rear of the model (microphone 2). Test conditions are nearly the same as for the example with the rotor and wing without the image plane (Fig. 9). The rotor blades ingesting the fountain produce a highly unsteady impulse in the acoustic pressure behind the model. The impulse was typically double sided (like a doublet), although single sided impulses (like a delta function) were also observed. Single and multiple impulses were observed throughout the record. The peak-to-peak amplitude varied from about 30 to about 140 Pa.

Fig. 13 shows an averaged power spectrum of the acoustic signal measured at the rear of the model (microphone 2). Frequencies from the 3rd to 20th harmonic form a hump in the spectrum similar to other

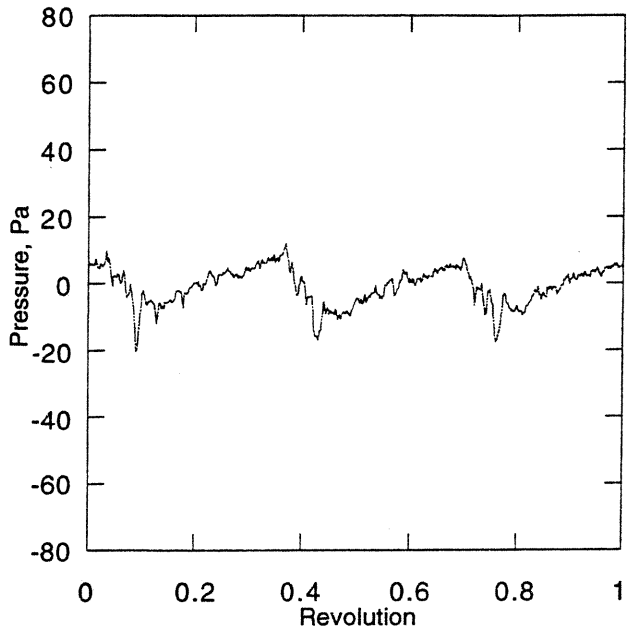

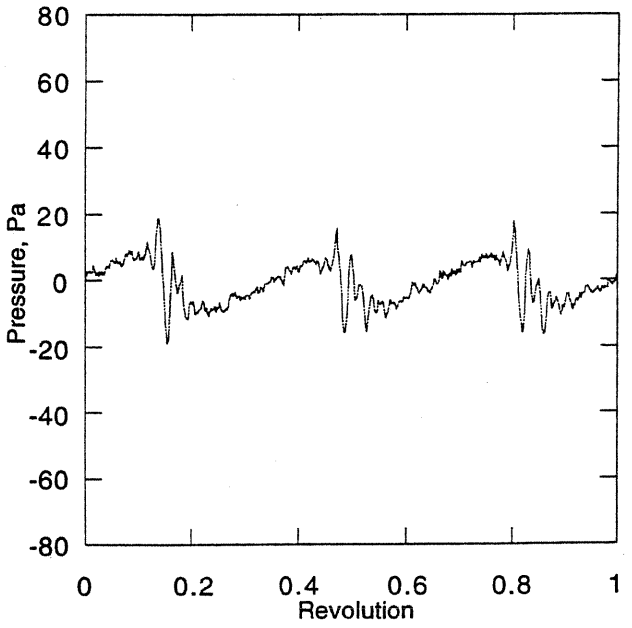

Fig. 9. Unaveraged time histories measured at the rear of the rotor with wing, microphone 2, C_{TE} = 0.0127, M_{tip} = 0.685 (a) low amplitude (b) high amplitude.

impulsive noise sources such as blade vortex interaction. The spectrum becomes broad band in nature above the 20th harmonic. Fig. 14 shows time histories of the OASPL, BL-SPL and FA-SPL computed for 250 revolutions. Levels and variation can be compared to the isolated rotor (Fig 4). BL-SPL nearly equaled OASPL since the high levels of the 7th to 12th blade passage harmonics contribute much of the energy to the OASPL in this very impulsive case. Acoustic pressure time histories measured in front of the model are again higher compared to the isolated rotor case. In front of the rotor, the measurements contain more high frequency energy than for the isolated rotor, but this energy is not organized in any recognizable way.

Figs. 15 and 16 show acoustic metrics as a function of effective thrust coefficient for locations in front (microphone 1) and at the rear

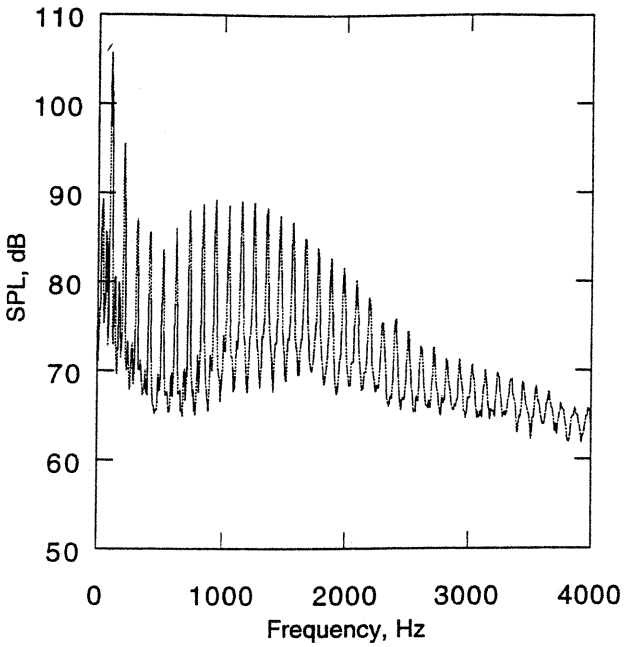

Fig. 10. Averaged power spectrum for the rotor with wing, microphone 2, C_{TE} = 0.0127, M_{tip} = 0.685, ΔF = 7.5Hz.

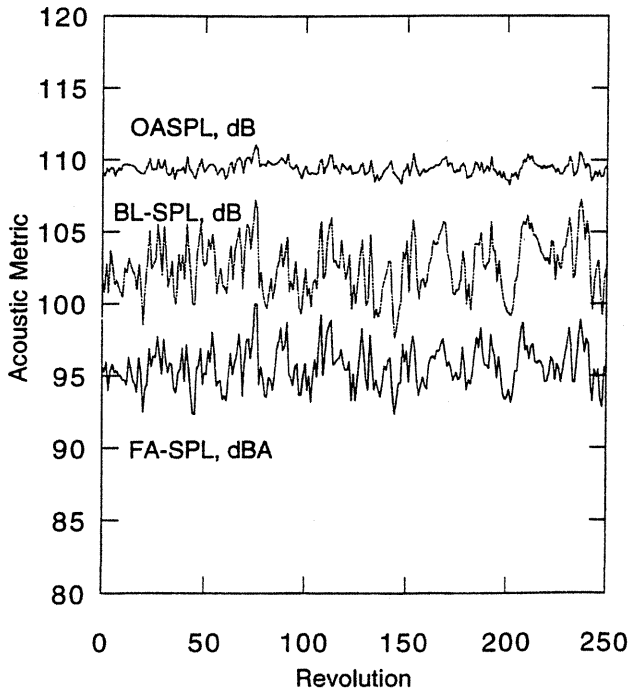

Fig. 11. Acoustic metrics for the rotor with wing, microphone 2, C_{TE} = 0.0127, M_{tip} = 0.685.

(microphone 2) of the model, respectively. The tip Mach number ranged from 0.684 to 0.686 and the wind was less than 5 knots. Acoustic metrics of the semi-span tilt rotor model are higher than OASPL and FA-SPL of the isolated rotor. Acoustic levels measured with the rotor and wing or the rotor and image plane are between levels measured for the isolated rotor and the tilt rotor configuration. In front of the model, the OASPL (Fig. 15a) is 1 to 2 dB higher and the FA-SPL (Fig. 15b) which

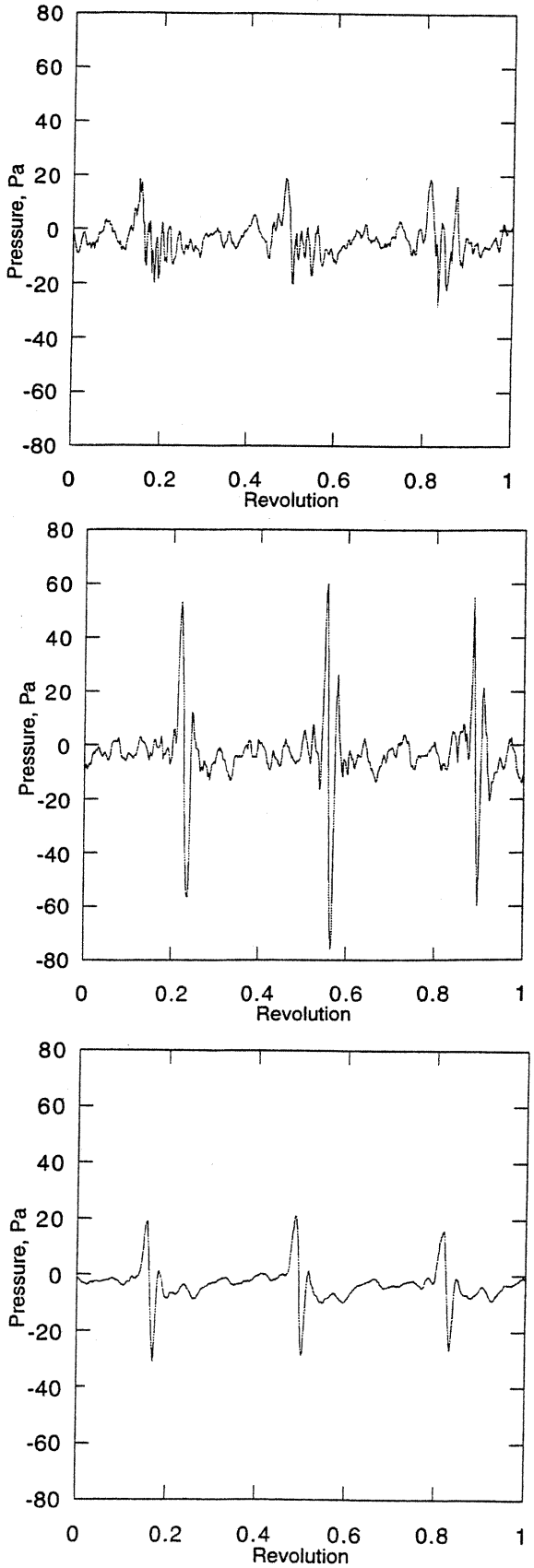

Fig. 12 Time histories measured at the rear of the rotor with wing and image plane, microphone 2, C_{TE} = 0.0124, M_{tip} = 0.685 (a) unaveraged and low amplitude (b) unaveraged and high amplitude (c) symchronous average of 60 revolutions.

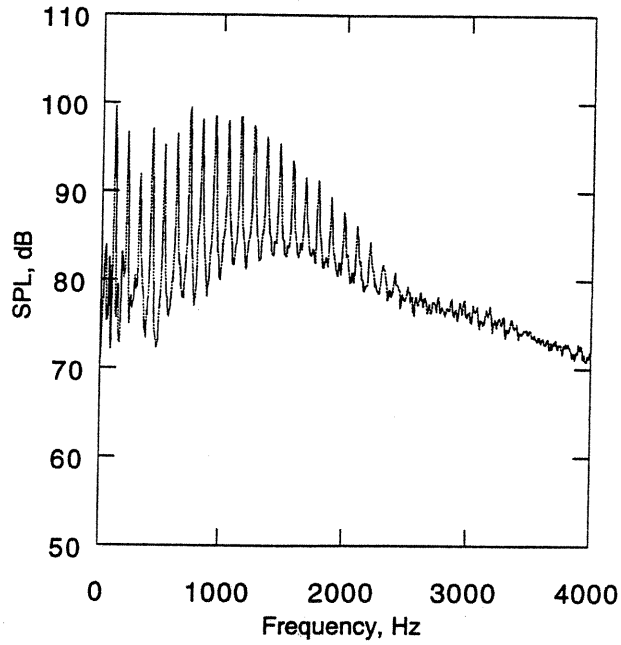

Fig. 13. Averaged power spectrum measured at the rear of the rotor with wing and image plane, C_{TE} = 0.0124, M_{tip} = 0.685, ΔF = 7.5 Hz

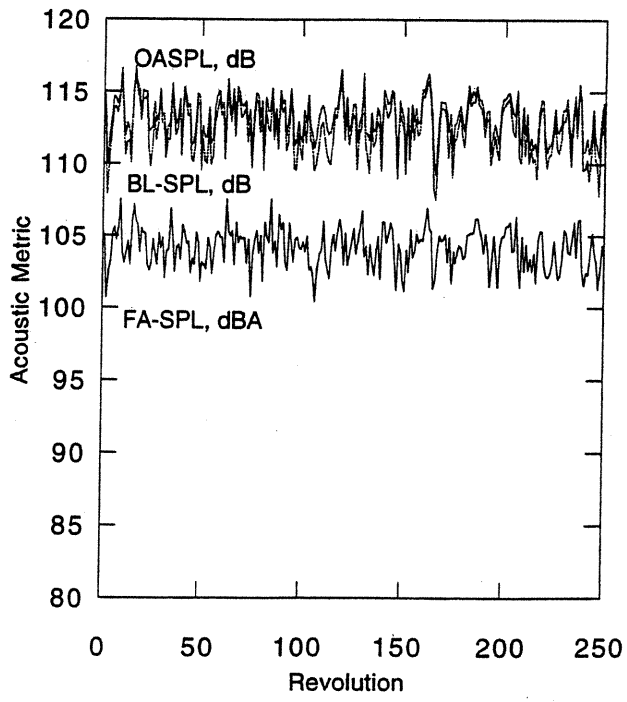

Fig. 14. Acoustic metrics for the rotor with wing and image plane, microphone 2, C_{TE} = 0.0124, M_{tip} = 0.685.

represents human perceptions is about 2 to 5 dBA higher for the aircraft model configuration than for the isolated rotor configuration. In the rear of the model, the OASPL (Fig. 16a) is about 5 to 7 dB higher and the FA-SPL (Fig 16b) is about 10 to 15 dBA higher, relative to the isolated rotor.

Configuration Changes to Wing

Many configurations were tested for their potential to reduce the

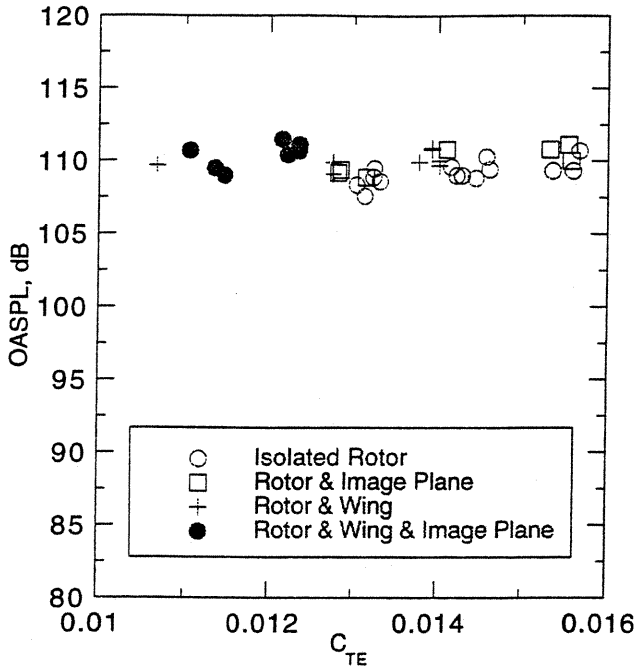

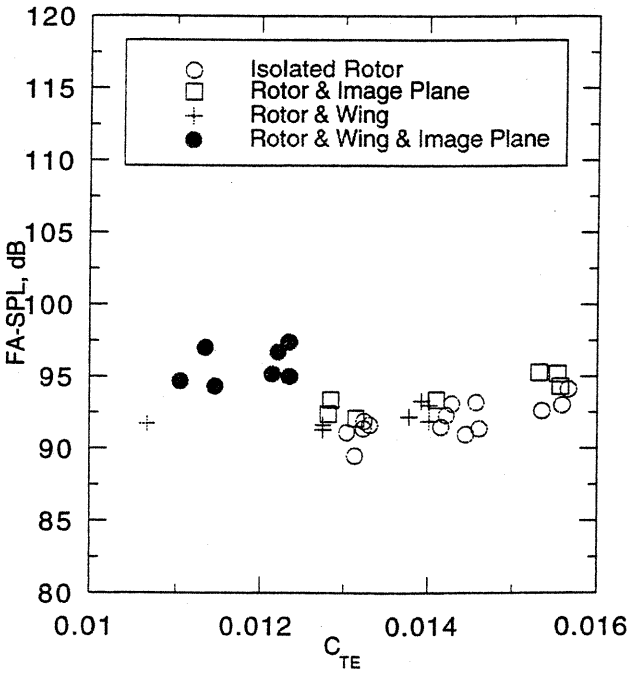

Fig. 15. Sound levels for rotor with and without wing and image plane in front of the model, microphone 1 (a) OASPL; (b) FA-SPL.

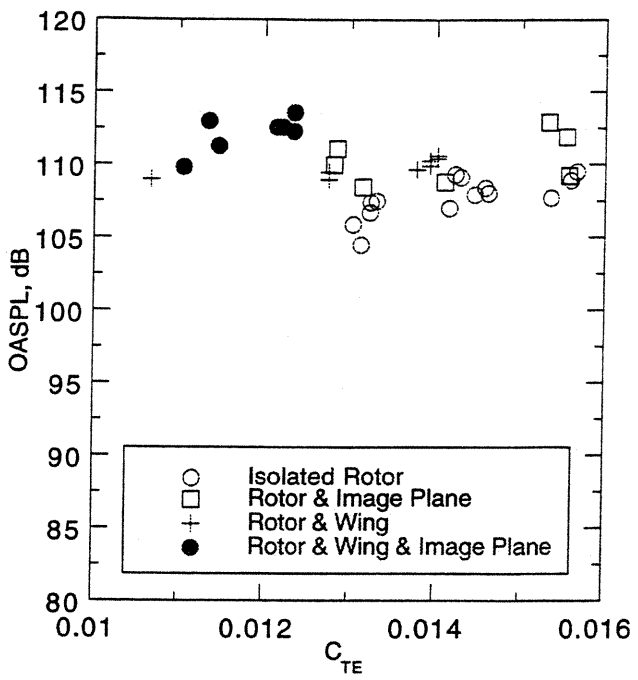

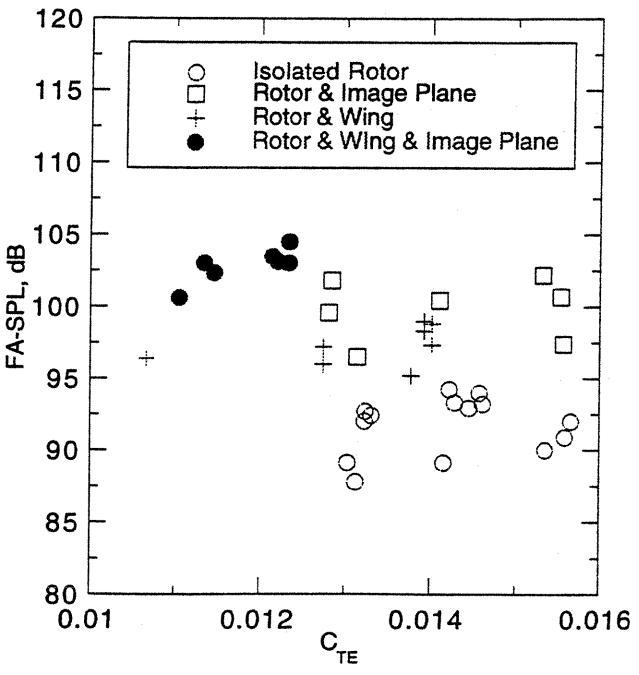

Fig. 16. Sound levels for rotor with and without wing and image plane at the rear of the model, microphone 2 (a) OASPL; (b) FA-SPL.

wing download. These configurations included increasing the rotor/wing separation, deflecting the flap, adding the nacelle, adding two vortex trapping plates on the upper surface and using upper surface blowing. Most changes produced no noticeable effect on the sound. However, increasing the wing span from 1.229 to 1.384 rotor radii reduced sound levels at both measurement locations (Fig. 17). The A-weighted sound pressure level adjusted to full-scale frequency decreased about 2 dB with the longer wing span. Adding two vortex trapping plates to the upper surface produced no noticeable effect in front of the model and produced a small reduction in noise to the rear of the model (Fig. 18).

Discussion

Results from this investigation reveal high noise levels to the rear of the model during hover operations. Average values of the A-weighted sound pressure level adjusted for full-scale frequencies reach 105 dB at 7 radii from the rotor. A tilt rotor must therefore avoid hovering near populated areas or a method to reduce this noise must be found.

During the testing, the Mach number was held constant and measurements were made only in low wind, below 5 kts. The thrust coefficient and the configurations were varied. Acoustic data is not available

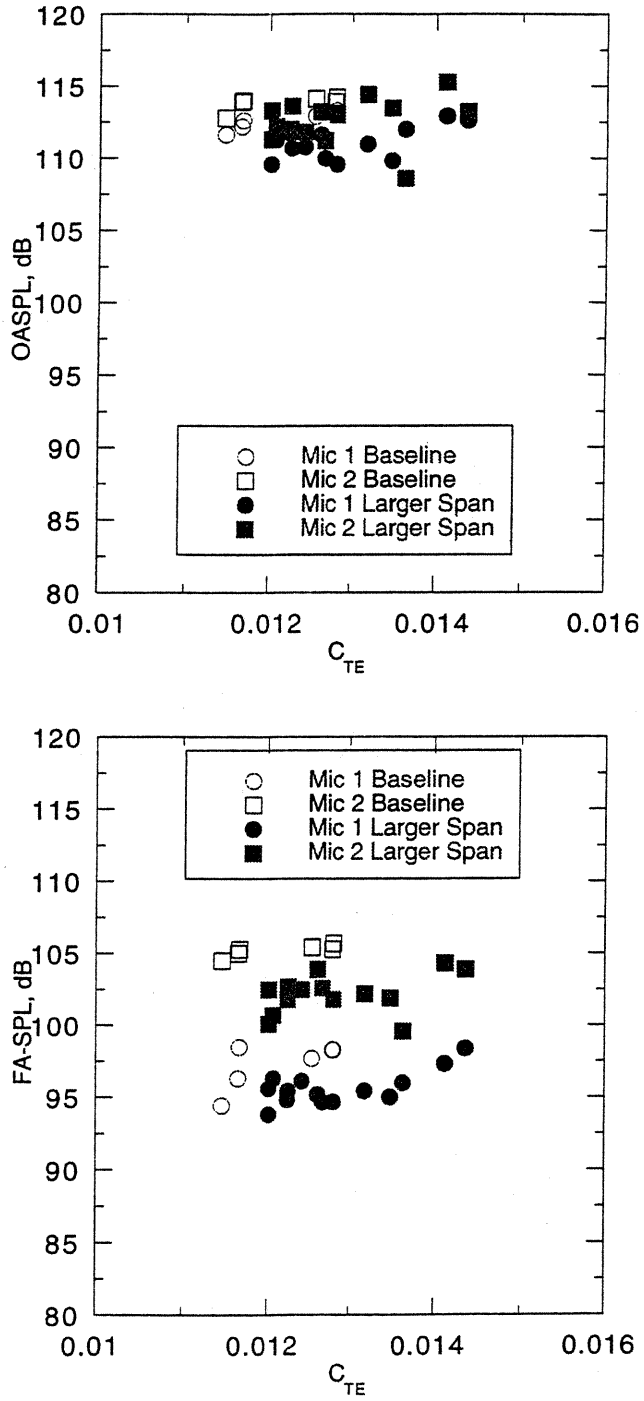

Fig. 17. Sound levels for baseline and configuration with larger wing span (a) OASPL; (b) FA-SPL.

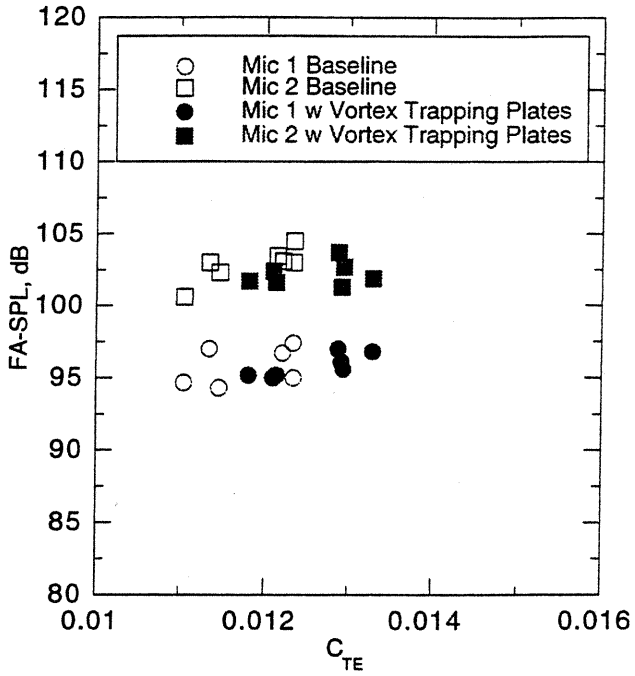

Fig. 18. Sound levels for baseline and configurations with vortex trapping plates, FA-SPL.

for the same thrust coefficients for all configurations resulting in less overlap than ideal for comparisons. We believe the lack of overlap for some comparisons does not affect the conclusions. For any particular configuration, the acoustic pressure level is expected to increase linearly with the thrust in the regime tested. The observed measurements follow this trend, so we believe valid conclusions can be made from this set of data.

Hover testing for tilt rotors at small-scale instead of full-scale probably has some effect on the acoustic measurements. The scale is not expected to affect the flow field's average characteristics and thus will not affect the average blade fountain interaction and resulting noise. If discrete vortical structure from the tip vortices are still present in the fountain, they will differ from full-scale tip vortices. Thus different, probably wider, impulses will radiate from the small-scale rotor as the rotor interacts with the vortices. The atmospheric turbulence obviously does not scale with the model size, so disturbances in the fountain flow related to atmospheric turbulence will have the wrong time and length scales for a small-scale model. This is expected to only change the number of revolutions of data required to obtain a stochastic time record.

Testing a semi-span tilt rotor does not fully model a full-span tilt rotor model. One difference, according to Ref. 3, is that for a full-span model the two fountains will mix and move from side to side, causing the fountain and associated noise to be more unsteady. Also, in this test, the image plane, due to limited size, did not provide a virtual image of the second rotor to the microphones. If a second rotor were present, the acoustic signal would contain impulses from both rotors, causing higher noise levels and more complex time histories. Fewer revolutions containing only low level impulses may occur, since when one rotor may not be ingesting the fountain, the other rotor may be ingesting the fountain and producing greater impulsive noise. To assess the effects of scale and semi-span modeling on the acoustics, noise measurements of a V-22 should be made and compared with measurements from this rotor.

Large and unsteady impulsive noise behind the aircraft resulted when the rotor blades ingested the fountain created by the presence of the wing and image plane. Smaller impulses occurred with only the image plane or only the wing present. Both of these intermediate configurations introduced small localized disturbances to the rotor inflow that produced small impulses as the rotor blades passed through them. In addition, some vortices may have shed off the edges of the image plane and been ingested into the rotor to produce noise.

The very unsteady nature of the impulsive noise measured behind the tilt rotor means individual revolutions of acoustic pressures are not representative. Long time records must be used to produce meaningful measurements. The standard practice of synchronously averaging acoustic pressure is not meaningful for this very unsteady data. For example,

the synchronous average of 60 revolutions generated a time history (Fig. 12c) with levels about equal to the minimum acoustic impulses (Fig. 12a). Most unaveraged impulses were larger, some over 4 times larger. Since the unsteady impulses do not sum constructively when synchronously averaged, the average amplitude exceeds the amplitude of the synchronous average. Also, the FA-SPL of the average power spectrum from Fig. 13 is 104.5 dB. The FA-SPL calculated from the time history of the synchronous average is 96.5 dB, a full 8 dB less. The average acoustic metrics provide good characterizations, but they lack detail.

To date, predictions of acoustic time histories of this impulsive noise have not accounted for the unsteadiness. For example, predictions in Ref. 10 are similar in appearance to the average time history in Fig. 12c. Levels from Ref. 10 can not be compared to this study due to differences in the aircraft and operating conditions. If calculations predict this 'average' time history, sound levels will be under predicted. To account for the variation in wave form and amplitude, a more sophisticated model of the fountain is needed in the acoustic predictions.

Most configurations tested for download reduction produced no effect on the measured noise levels, although increasing the span reduced the noise slightly. This effect may occur because there is more space between the rotor and image plane, so less of the fountain may be ingested into the rotor. Other configurations probably produced no significant change in the fountain and thus no change in the noise.

To reduce the loud, annoying impulsive noise from the blade fountain interaction either the sensitivity of the blade to disturbances needs to decrease or the fountain needs to be greatly reduced or the fountain needs to be deflected away from the rotors. To date researchers have not had much success reducing the sensitivity of rotor blades to disturbances. Some of the download reduction techniques have reduced the download, but they have not reduced the fountain enough to significantly reduce the noise. A flow control device that produces an asymmetry above the fuselage where the flows from the two rotor wakes meet may be able to direct the flows forward and/or aft instead of up. A retractable diagonal fence above the fuselage might reduce the noise in this way. Polak and George tested a diagonal fence and reported a reduction of about 3 dB in Ref. 15.

Conclusions

The following conclusions are based on the small-scale, semi-span test of a hovering tilt rotor:

1. Noise from a hovering tilt rotor exceeds noise from an isolated rotor operating at the same conditions. The full-scale frequency adjusted A-weighted sound pressure level is about 2 to 5 dBA higher in front of the model and about 10 to 15 dBA higher to the rear of the model. Most of the increase is caused by the rotor blades interacting with the unsteady fountain. The increased noise is impulsive.
2. The impulsive noise from the rotor ingesting the fountain is very unsteady. Some impulses in an 8 second data record are over 4 times larger than others. Long time records are needed to produce reliable acoustic metrics. Synchronous averaging of the acoustic pressures gives a false representation of the noise.
3. Acoustic measurements contain significant scatter, up to 5 dB, which was not attributed to any other variable measured. Many data records are needed to compensate for the scatter.
4. Increasing the wing semi-span from 1.229 to 1.384 rotor radii reduced the full-scale frequency adjusted A-weighted sound pressure level about 2 dB.
5. Increasing the rotor/wing separation distance, deflecting the flap, adding the nacelle and using upper surface blowing produced no noticeable effect on the acoustic measurements in this test.

References

[1] McVeigh, M. A., "The V-22 Tilt-Rotor Large-Scale Rotor Performance/Wing Download Test and Comparison with Theory," 11th European Rotorcraft Forum, London, England, Sept. 1985.

[2] Felker, F. F. and Light J. S., "Aerodynamic Interaction Between a Rotor and Wing in Hover," *Journal of the American Helicopter Society,* Vol. 33, (2), April 1988.

[3] Coffen, C. D., George, A. R., Hardinge, H., and Stevenson, R., "Flow Visualization and Flow Field Measurements of a 1/12 Scale Tilt Rotor Aircraft in Hover," American Helicopter Society and Royal Aeronautical Society International Technical Specialists Meeting on Rotorcraft Acoustics and Rotor Fluid Dynamics, Valley Forge, PA, Oct. 1991.

[4] McVeigh, M. A., Grauer, W. K., and Paisley, D. J., "Rotor/Airframe Interactions on Tiltrotor Aircraft," *Journal of the American Helicopter Society,* Vol. 35, (3), July 1990.

[5] Coffen, C. D., "Tilt Rotor Hover Aeroacoustics," NASA CR 177598, June 1992.

[6] George, A. R., Smith, C. A., Maisel, M. D., and Brieger, J. T., "Tilt Rotor Aircraft Aeroacoustics," American Helicopter Society 45th Annual Forum, Boston, MA, May 1989.

[7] Conner, D. A. and Wellman, B., "Hover Acoustic Characteristics of the XV-15 with Advanced Technology Blades," *AIAA Journal of Aircraft,* Vol. 31 (4) July 1994.

[8] Hoad, D. R., Conner, D. A., and Rutledge, C. K., "Acoustic Flight Experience with the XV-15 Tiltrotor Aircraft with the Advanced Technology Blades (ATB)," AIAA 14th Aeroacoustic Conference, Aachen, Germany, May 1992.

[9] Coffen, C. D. and George, A. R., "Analysis and Prediction of Tilt Rotor Hover Noise," American Helicopter Society 46th Annual Forum, Washington D. C., May 1990.

[10] Rutledge, C. K., Coffen, C. D., and George, A. R., "A Comparative Analysis of XV-15 Tiltrotor Hover Test Data and WOPWOP Predictions Incorporating the Fountain Effect," American Helicopter Society and Royal Aeronautical Society International Technical Specialists Meeting on Rotorcraft Acoustics and Rotor Fluid Dynamics, Valley Forge, PA, Oct. 1991.

[11] Coffen, C. D. and George, A. R., "Tilt Rotor Broadband Hover Aeroacoustics," *ASME Journal of Fluids Engineering,* Dec. 1993.

[12] Light, J. S., Stremel P. M., and Bilanin A. J., "Wing Download Reduction Using Vortex Trapping Plates," American Helicopter Society Aeromechanics Specialist Conference, San Francisco, CA, Jan. 1994.

[13] Watts, M. E., "ALDAS User's Manual." NASA TM 102381, April 1991.

[14] Hagen, M. J., Yamauchi, G. K., Signor, D. B., and Mosher, M., "Measurements of Atmospheric Turbulence Effects on Tail Rotor Acoustics," NASA TM, 108843, Sept. 1994.

[15] Polak, D. R. and George, A. R., "Flowfield and Farfield Acoustic Measurements from a Scaled Tiltrotor in Hover," AIAA 16th Aeroacoustic Conference, Munich, Germany, June 1995.